Egypt. J. Chem. Vol. 67, SI: M. R. Mahran, pp. **1031 - 1036** (2024)

Egyptian Journal of Chemistry

http://ejchem.journals.ekb.eg/

Electrochemical Behaviour of Dissimilar Joints from Monel400 and AISI 1020 Carbon Steel

Mahmoud Abbas[1], Mohamed M.Z. Ahmed[2], Hamed.A.Abdel-Aleem[3], Nada Azab[4]

[1] *Suez University. Petroleum and Mining Engineering Faculty, Department of Metallurgical and Materials Engineering, Assalam City, Suez, P.O. Box 43533, Egypt.*

[2] *mohamed.zaky@suezuniv.edu.eg*

[3]*(CMRDI) Central Metallurgical Research and Development Institute, Helwan, 11722 Egypt*

[4] *(SOPC) Suez Oil Processing Co. Suez, P.O. Box 100 Egypt.*

Abstract

Nickel–copper alloys are commonly utilized for their corrosion resistance in electrochemical applications, marine engineering, and various other fields. The corrosion resistance of these metal combinations significantly improves with higher nickel substance. Therefore, in this study, the impact of a 10% HCl solution on Monel400 and AISI 1020 carbon steel welded joints produced by Friction Stir Welding and Shielded Metal Arc Welding, was examined. The microstructures of the weld were analysed using both Scanning Electron Microscopy (SEM) and optical microscopy. Corrosion behavior was assessed through cyclic and potentiodynamic polarization tests, with specimens submerged in a 10% HCl solution for 30 days. The study revealed a dealloying phenomenon, specifically nickel leaching from Monel 400, referred to as denickelation. Results showed that corrosion rates of Monel400- 1020 Carbon steel joint with FSW, and SMAW welding using ENiCu-7 and ENiCrFe-3 electrodes were respectively 20. mpy 26 mpy and 30 mpy, the pitting potential was about 1600V in FSW specimen and 1500V in SMAW specimen.

Keywords Friction Stir Welding (FSW), Fusion Welding, AISI 1020 carbon steel, Monel 400, electrochemical measurements, Denickelation.

1. Introduction

Monel400 is broadly utilized within the desalination industry and other marine designing divisions due to its composition, which incorporates 60-70% nickel, 20-29% copper, and little sums of iron, manganese, silicon, and carbon. This alloy offers exceptional corrosion resistance in various environments, including the atmosphere-, seawater, and a range of acidic and alkaline media. Its combination of corrosion resistance, ductility, and workability makes Monel 400 highly desirable for numerous other applications.

According to its exceptional properties, Monel 400 was commonly utilized for both oxidizing and reducing environments, as well as in marine manufacturing, power plants, and also chemical plants, and the manufacture of valves, pumps, boilers, and other heat exchangers. [1-8].

Friction stir welding (FSW) is a solid-state joining technique that employs a non-consumable tool to bond two adjacent workpieces without melting their material [9-10]. The heat required for the process is produced by friction between the rotating tool and the workpiece material, creating a softened zone near the FSW tool. As the tool moves along the joint, it mechanically mixes the two pieces of metal and forges the heated, softened material under the pressure exerted by the tool.

Shielded metal arc welding (SMAW), commonly referred to as manual metal arc welding (MMA or MMAW), flux shielded arc welding [11], or informally as stick welding, is a manual arc welding method in which a consumable electrode coated with flux is used to create the weld.

In this work, joints among Monel400 and AISI1020 carbon steel with different welding techniques were exposed to highly corrosive media such as HCl to investigate and compare their different reactions. Previous research by Sadek and Abbas [12] studied dissimilar joints between steel and Monel400 created through fusion welding techniques using two different types of filler electrodes.

This work aims to evaluate the corrosion resistance of bimetallic welded joints between Monel400 and AISI1020 carbon steel, created using both the Friction

*Corresponding author e-mail: Nada.m.azab@gmail.com

Receive Date: 24 August 2024, Revise Date: 20 September 2024, Accept Date: 23 September 2024

DOI: 10.21608/ejchem.2024.314211.10255

Stir Welding (FSW) process and Shielded Metal Arc Welding (SMAW) process.

2. Experimental Procedure

2.1 Materials

2.1.1 AISI 1020 Carbon Steel

The AISI 1020 Carbon Steel is delivered from EZZ El-Dekhela Steel Company, Egypt.

Mechanical characteristics and the chemical compositions of AISI 1020 Carbon Steel are given in tables (1-2).

Table (1) AISI 1020 Carbon Steel Chemical composition delivered from Ezz el Dehkela steel co. (wt%)

C	Mn	Si	P	S	Fe
0.193	0.652	0.22	0.006	0.002	Balance

Table (2) AISI 1020 Mechanical properties

Tensile Strength, Yield	Tensile Strength, Ultimate	Elongation at Break
310 MPa	450 MPa	26%

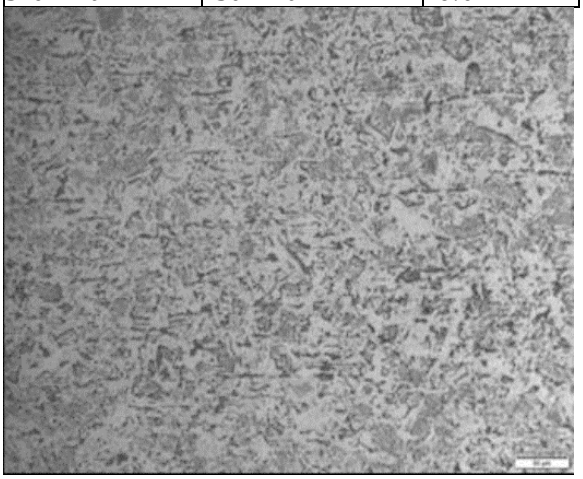

Fig. 1 Microstructure of AISI 1020 Carbon Steel

The shown microstructure of AISI1020 carbon steel is composed of both ferrite and pearlite at which the dark area is Pearlite while the white area is ferrite

2.1.2 Monel 400

The Monel 400 metal is delivered from Suez Oil Processing Company in Suez, Egypt.

Mechanical characteristics and the chemical compositions of Monel 400 are given in tables (3-4).

Table (3) Monel400 Chemical composition using XRF in SOPC (wt%)

Ni	Cu	Fe	Mn	Mg	Co	Others
65.5	29.7	1.36	1.23	1.1	0.57	0.57

Table (4) Monel 400 Mechanical properties.

Tensile Strength, Yield	Tensile Strength, Ultimate	Elongationat Break
240 MPa	550 MPa	40%

Fig.2 Microstructure of Monel400

Figure shows Monel 400 is characterized by equiaxed grains of ɣ Solid Solution.

2.2 Friction Stir Welding (FSW) process

Friction Stir Welding was chosen due to its high range of advantages like energy efficient, environment friendly, and versatile, also it is used to join high-strength alloys and other metallic alloys that are harder to weld by conventional fusion. welding Materials used in this work were 3 -mm thickness Monel400 and AISI 1020 Carbon Steel.

The FSW process was conducted at rotational speeds of 200, 250, and 400 rpm, with navigate speeds of 50 and 100 mm/min. The plates were joined in a butt-weld setup, with a plunge profundity of 3 mm connected by FSW. To make a microstructural analysis, specimens were cut opposite to the FSW course. Specimens for optical microscopy and SEM investigations were prepared following ASTM E-3 [13] and ASTM E-2014 [14] standards. The AISI 1020 carbon steel and Monel 400 sides were etched using 2% nital and Marble's reagent, respectively [15], and examined using optical microscopy (OM).

FSW depends on the plastic flow of materials created by a non-consumable turning apparatus embedded into the joint to be welded. The warm required to initiate the essential plastic flow for joint arrangement is primarily generated at the interface between the device and the workpiece. This process is impacted by components such as rotational speed, welding speed, axial stack, and apparatus shoulder diameter (D).

Hattel and Schmidt enhanced an expository show for warm era in FSW. A key distinction of this model compared to previous ones is the incorporation of a parameter called slip rate (δ), which ranges from 0 to 1. A slip rate of 0 indicates a sliding contact condition, while a slip rate of 1 indicates a sticking contact condition. According to (Mishra and Ma [16]; Mishra and Mahoney) even though it has been detailed that the heat input created by the apparatus pin can account for up to 20% of the whole heat input, the terms related to

the apparatus pin are omitted in this investigation to disentangle the method.

Based on this model, Equation 1 represents the power (Q) generated during FSW as a function of rotational speed (ω) and diameter of the tool shoulder (D), assuming that the (shear) yield stress (τy), coefficient of friction (μ), rate of slip (δ), and contact pressure (p) are uniformly distributed across the interface.

$$Q = \frac{2}{3}\pi\left[\omega\left(\delta.\tau_y + (1-\delta)\mu.p\right)\right]\left(D/2\right)^3 \quad \text{.....[17]}$$

For the FSW process, the heat input calculated using Equation 1 was found to be 177.66 watts.

Fig. 3 and 4 display the cross-sectional area for the produced FSW. Generally, four unmistakable locales are displayed after FSW: the stirred zone (SZ) or which is called the nugget zone, the thermomechanical affected zone (TMAZ), the heat-affected zone (HAZ), and the base metal (BM).

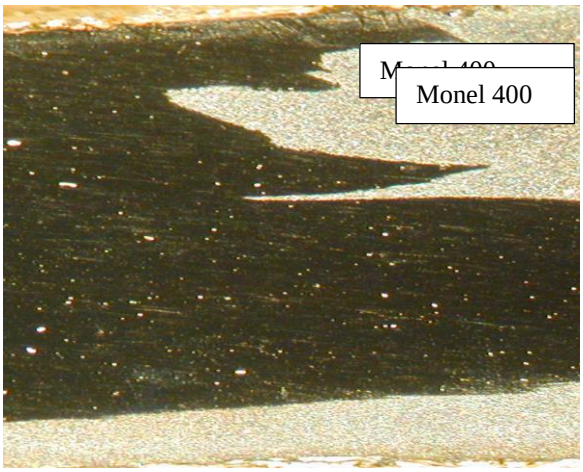

Fig. 3 cross-sectional area of the Joint in whick steel (Dark area) inside Monel400 (light area)

.

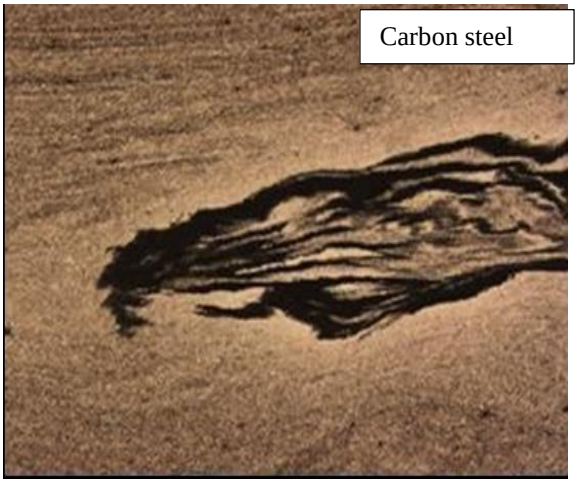

Fig. 4 cross-sectional area of produced FSW joint showing carbon steel (dark area) inside Monel 400 (light area)

2.3 Shielded Metal Arc Welding

In this study, the dissimilar materials used were 3-mm thickness AISI1020 carbon steel and Monel 400. The chemical composition and mechanical characteristics of AISI 1020 carbon steel and Monel 400 have been detailed previously. The specimens were welded using two electrodes: ENiCrFe-3 and ENiCu-7, as they are most recommended electrods for such weldments according to Sadek and Abbas [9].

Their chemical and mechanical analysis provided in Table 5-6

Table (5): Chemical analysis for welding electrodes [9]

Chemical composition, %	ENiCu-7	ENiCrFe-3
Ni+Co	62	Bal
Cu	Bal	0.1
Mn	4	7.75
Fe	2.5	7.5
Si	1	0.5
C	0.15	0.05
S	0.015	0.008
Al	0.75	---
Ti	1	0.04
Nb+Ta	---	1.75
Cr	---	14

Table (6): Mechanical properties for welding electrodes

	ENiCu-7	ENiCrFe-3
Tensile Strength	75,000 psi	85,000 psi
Yield Strength	51,500 psi	54,000 psi
Elongation	38%	35%

2.3.1 Welding Procedure

Base metals were prepared as strips with dimensions of 30 x 20 x 3 mm. The Shielded Metal Arc Welding (SMAW) process was used for this work, and the joint configuration is depicted in Figure 5.

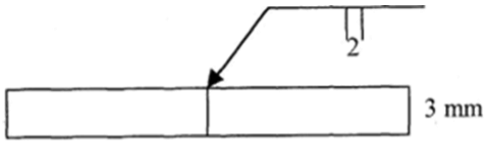

Fig. 5 Joint design

The joints were held in place until they cooled, after which the slag was removed. The ideal welding parameters for SMAW Welding of Monel400 and AISI1020 carbon steel are listed in Table 7.

Table (7): best parameters for fusion welding:

Current, A	80
Travel speed, (mm/s)	3.75
Voltage, V	12
Polarity	DCSP
Groove position	Flat

3. Results and Discussion

3.1 Microstructural evolutions

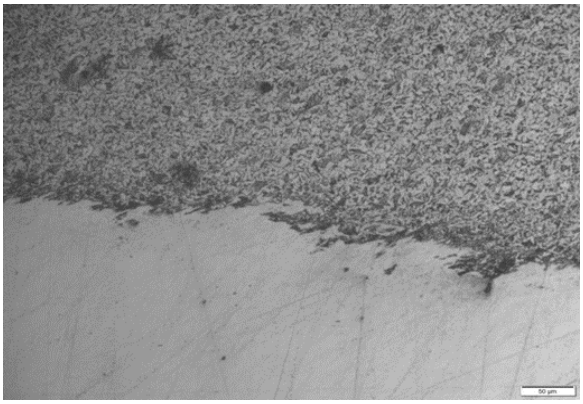

Fig. 6 Microstructure of Monel in HAZ

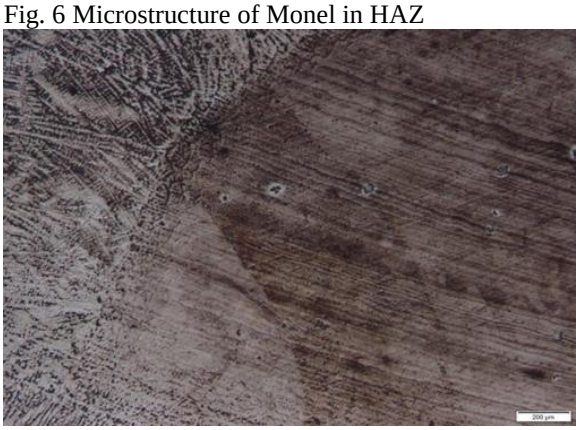

Fig. 7 Microstructure of Carbon steel in HAZ

Figures 6 and 7 shows the microstructure of both Monel400 and AISI 1020 Carbon Steel in HAZ showing the interference between Monel 400 and AISI 1020 carbon steel Obviously, there is a desirable mix of two alloys in the SZ

4.Corrosion Testing

The specimen dimensions 3*5*30 mm for Corrosion Testing, the specimen preparation was carried out according to ASTM E-3 [14] with final cleaning in an ultrasonic cleaner.

A mounting was applied to be over the specimens except for the area on the weld for each specimen.

4.1 potentiodynamic polarization

Electrochemical tests were conducted using the potentiodynamic testing method in accordance with ASTM G 5 [17], which provides standard procedures for potentiostatic and potentiodynamic anodic polarization measurements. Additionally, the guidelines from ASTM G 3 [18] were followed.

A graphite rod was used as counter electrode and the reference electrode was saturated calomel electrode (SCE) K/KCL type.

The electrochemical testing of Monel400 and AISI 1020 carbon steel was conducted using Potentiodynamic method with a potentiostat connected to a PC. The specimens were polarized in a 10% HCl solution prepared from analytical grade HCl and distilled water

The Potentiostat was held using VersaSTAT3 with a Versa studio electrochemical software.

4.2CyclicPotentiodynamic polarization (CPP)

To determine pitting potential of the specimen's tests were operated in 10%HCl solution from an initial potential of -2V with respect to OCP to a final potential of -2V with respect to the Saturated Calomel Electrode keeping the vertex potential to be -2V with scan rate of 3mV.S-1and the corresponding current was recorded.

In other method, the specimens were submerged in the Corroding solution for about 2 weeks.

Corrosion rate of each specimen was determined by Tafel extrapolation technique.

The potentiodynamic polarization results and corrosion rates for the Monel 400 and AISI 1020 joints in 10% HCl are presented in Table 8.

Table (8) Results for corrosion test

Specimen	Corrosion rate
Monel400-Monel400 FSW	13 mpy
Monel400 -Carbon Steel FSW	20.3 mpy
Monel400 -Carbon Steel (ENiCu-7)	26.15 mpy
Monel400 -Carbon Steel (ENiCrFe-3)	30.83 mpy

Polarization curves are shown in Figures 8 a and b below.

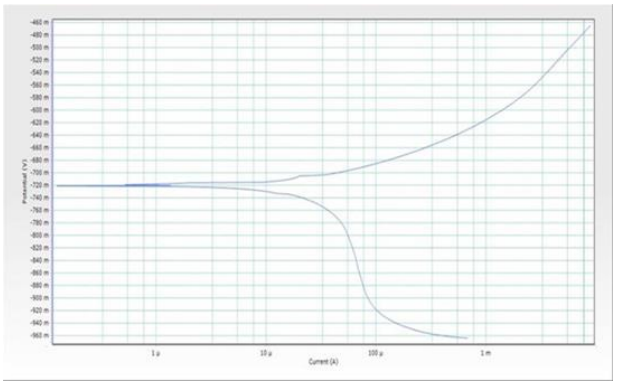

(a)

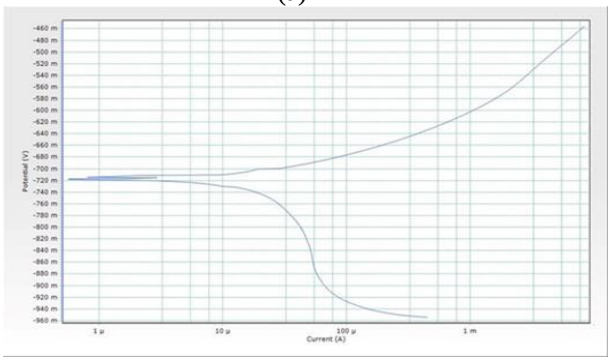

(b)

Fig. 8 Polarization curves (a) For FSW
(b) For SMAW

Cyclic polarization method is commonly used to evaluate metals and alloys that achieve their corrosion resistance through the formation of a thin passive film. Cyclic polarization curves of Friction stir welded specimens immersed in HCl and Shielded metal arc welded specimen

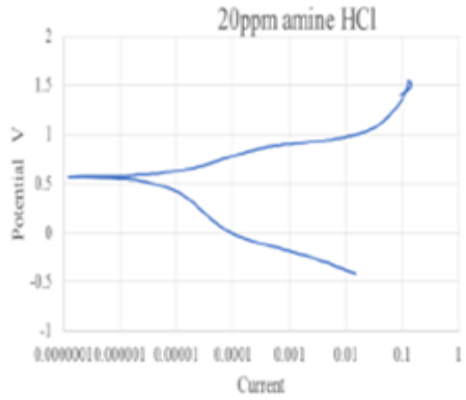

(a)

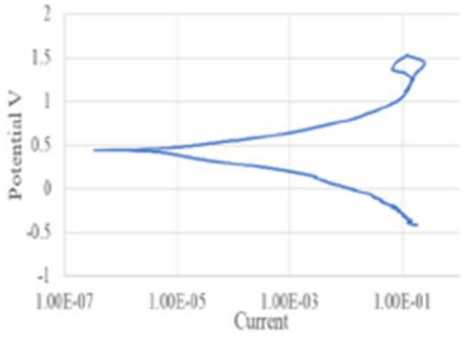

(b)

Fig. 9 (a) Cyclic potential of the FSW specimen in 10% HCl, while (b) depicts the cyclic potential of the SMAW.

The specimens were submerged in 10% HCl for 30 days. After removing the solution, Monel 400 exhibited a reddish appearance, and a new phenomenon, known as denickelation, was observed. This phenomenon is a type of dealloying.

Fig. 10 showing Denickelation

Denickelation is a type of corrosion in which nickel is leached out of its alloys. This process typically occurs in copper-nickel alloys after prolonged exposure to seawater or other aquatic environments.

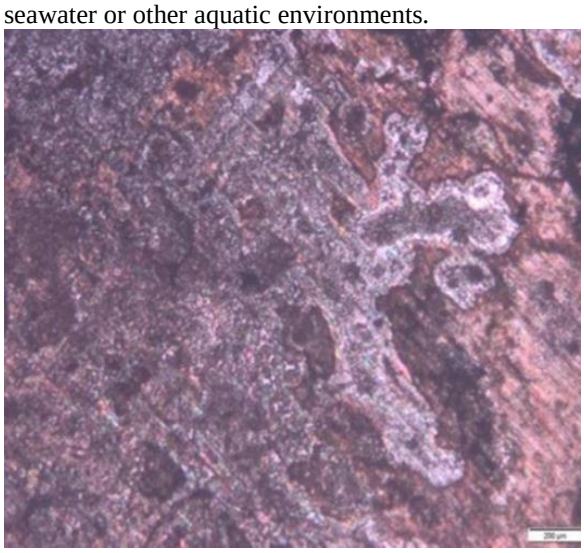

(a)

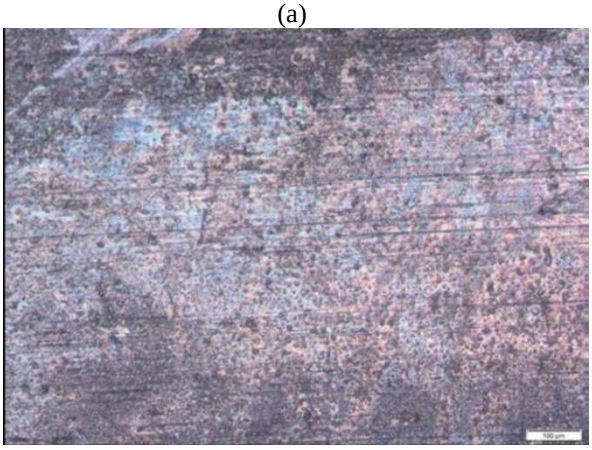

(b)

Fig. 11 Microstrucure showing Denickelation in **(a)** SMAW specimen **(b)** FSW specimen

5. Conclusions

- The FSW process, using the selected parameters, produced high-quality welds without cracks or cavities between Monel 400 and AISI 1020 carbon steel.
- The ENiCrFe-3 electrode showed better results due to its chromium content (about 14%) so (Cr_2O_3) (protective layer) is formed.
- Corrosion is most severe at the weld nugget area and the forward side due to uneven weld microstructures and precipitate distribution, with lighter corrosion observed at the return side.
- Pitting in Monel alloys results from denickelation , where the breakdown of the oxide film during FSW promotes anodic reactions.

- Denickelation was found to be more severe in SMAW compared to FSW, attributed to the difference in heat input.

6. References

1. T. Hodgkiess, G. Vassiliou “Complexities in the erosion corrosion of copper-nickel alloys in saline water” Desalination, Doi : https://doi.org/10.1016/j.desal.2005.03.037, Volume 183, Issues 1–3, Pages 235-247, 1 November (2005)
2. E.M. Sherif, A.A. Almajid, A.K. Bairamov, E. Al-Zahrani “Corrosion of Monel-400 in Aerated Stagnant Arabian Gulf Seawater after Different Exposure Intervals” International Journal of Electrochemical Science, Doi: https://doi.org/10.1016/S1452-3981(23)18418-5, Volume 6, Issue 11, Pages 5430-5444, November (2011)
4. J.A. Ali, J.R. Ambrose “The relationship between copper component dissolution kinetics and the corrosion behaviour of monel-400 alloy in de-aerated NaCl solutions” Corrosion Science, Doi: https://doi.org/10.1016/0010-938X(92)90169-4 , Volume 33, Issue 7, Pages 1147-1159, July (1992)
5. C.J. Semino, P. Pedeferri, G.T. Burstein, T.P. Hoar “The localized corrosion of resistant alloys in chloride solutions” Corrosion Science, Volume 19, Issue 7, Pages 1069-1078, (1979)
6. S.S. Prabha, R.J. Rathish, R. Dorothy, G. Brindha, M. Pandiarajan, A. Al-Hashem, S. Rajendran “Corrosion problems in petroleum industry and their solution”. Eur Chem Bull 3(3):300–307, (2014)
7. S. Hettiarachchi, T.P. Hoar “Morphological studies of some high nickel alloys in the region of the breakdown of passivity” Corrosion Science, Volume 19, Issue 12, Pages 1059-1067, (1979)
8. V.K. Gouda, I.Z. Selim, A.A. Khedr, A.M. Fathi “Pitting Corrosion Behaviour of Monel-400 Alloy in Chloride Solutions” Material. Science Technology, Doi: https://www.jmst.org/EN/Y1999/V15/I03/208 , 15 208. (1999).
9. Li, Kun; Jarrar, Firas; Sheikh-Ahmad, Jamal; Ozturk, Fahrettin "Using coupled Eulerian Lagrangian formulation for accurate modeling of the friction stir welding process". Procedia Engineering. 207: 574–579. Doi:10.1016/j.proeng. 2017.10.1023. (2017).
10. "Welding process and its parameters - Friction Stir Welding". www.fswelding.com. Archived from the original on 2020-07-22. Retrieved 2017-04-22.(2020)
11. Houldcroft, P. T. [1967]. "Chapter 3: Flux-Shielded Arc Welding". Welding Processes. Cambridge University Press. p. 23. ISBN 978-0-521-05341-9. (1973)
12. A.A. SADEK, M. ABASS “Investigation of Dissimilar Joints Between Low Carbon Steel and Monel 400” trans JWRL, Vol. 29, No.1, (2000)
13. ASTM E-3, “Standard Guide for Preparation of Metallographic Specimens”,1-11., (2011).
14. ASTM E-2014, “Standard Guide on Metallographic Laboratory Safety”, 1- 7, (2017).
15. K. D. Ramkumar, V. Joshi, S. Pandit, M. Agrawal, O. S. Kumar, S. Periwal, M. Manikandan, N. Arivazhagan” Investigations on the microstructure and mechanical properties of multi-pass pulsed current gas tungsten arc weldments of Monel 400 and Hastelloy C276” Materials and Design 64 775-782. (2014)
16. R.S. Mishra a, Z.Y. Ma b “Friction stir welding and processing” Volume 50, Issues 1–2, Pages 1-78, 31 August (2005)
17. ASTM G5–94, “Standard reference test method for making potentiostatic and potentiodynamic anodic polarization measurements”, (2004).
18. ASTM G3–89, “Standard practice for conventions applicable to electrochemical measurements in corrosion testing”, (2004).